

Understanding the Inductances

We have identified six different inductances (or reactances) for characterizing machine dynamics. These are:

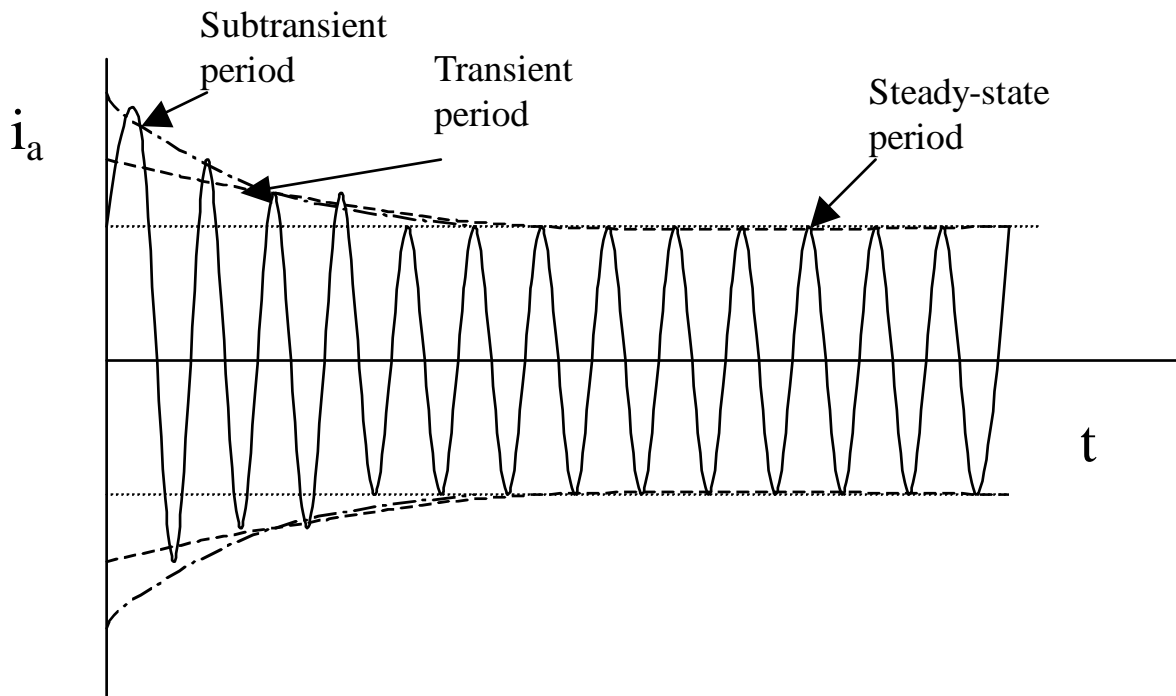
L_d, L_q (synchronous), L'_d, L'_q (transient), L''_d, L''_q (subtransient)

Once we obtain L_d and L_q , together with the rotor winding self inductances L_F, L_D, L_G , and L_Q , and the mutual inductances L_{AG} and L_{AQ} , then we may obtain the other four inductances through the following relations that we developed in class:

$$L'_d = L_d - \frac{L_{AD}^2}{L_F} \qquad L'_q = L_q - \frac{L_{AQ}^2}{L_G}$$

$$L''_d = L_d - \frac{L_D + L_F - 2L_{AD}}{\frac{L_F L_D}{L_{AD}^2} - 1} \qquad L''_q = L_q - \frac{L_Q + L_G - 2L_{AQ}}{\frac{L_G L_Q}{L_{AQ}^2} - 1}$$

There are two pictures that may be helpful in understanding these inductances. One comes from Kundur's book, Fig. 3.27, pg. 109, which characterizes the "phase a" stator current for a three-phase fault occurring at the machine terminals. This picture, drawn neglecting the stator transients (since they are very fast), is given below:



Note here that the subtransient period lasts for only a few cycles, during which the amplitude decays rapidly; the transient period spans a longer time frame, during which the amplitude decays more slowly; in the steady-state period, the amplitude is constant. The subtransient, transient, and synchronous inductances correspond to the subtransient, transient, and steady-state time periods, respectively.

The second helpful picture is Figure 15 out of Kimbarks' volume III (pg 26). This figure is key to understanding the inductances, what they represent, and their relative magnitudes (remembering their relative magnitudes is especially helpful in identifying inappropriate data).

Kimbark's picture identifies the flux paths for various reactances of a salient pole machine. The figures in this picture are drawn for the situation (the "thought-experiment") that we considered in deriving the inductances. In this situation, the rotor circuits were all closed but not excited (e.g., $v_f=0$), the rotor is turned forward at synchronous speed, and the stator

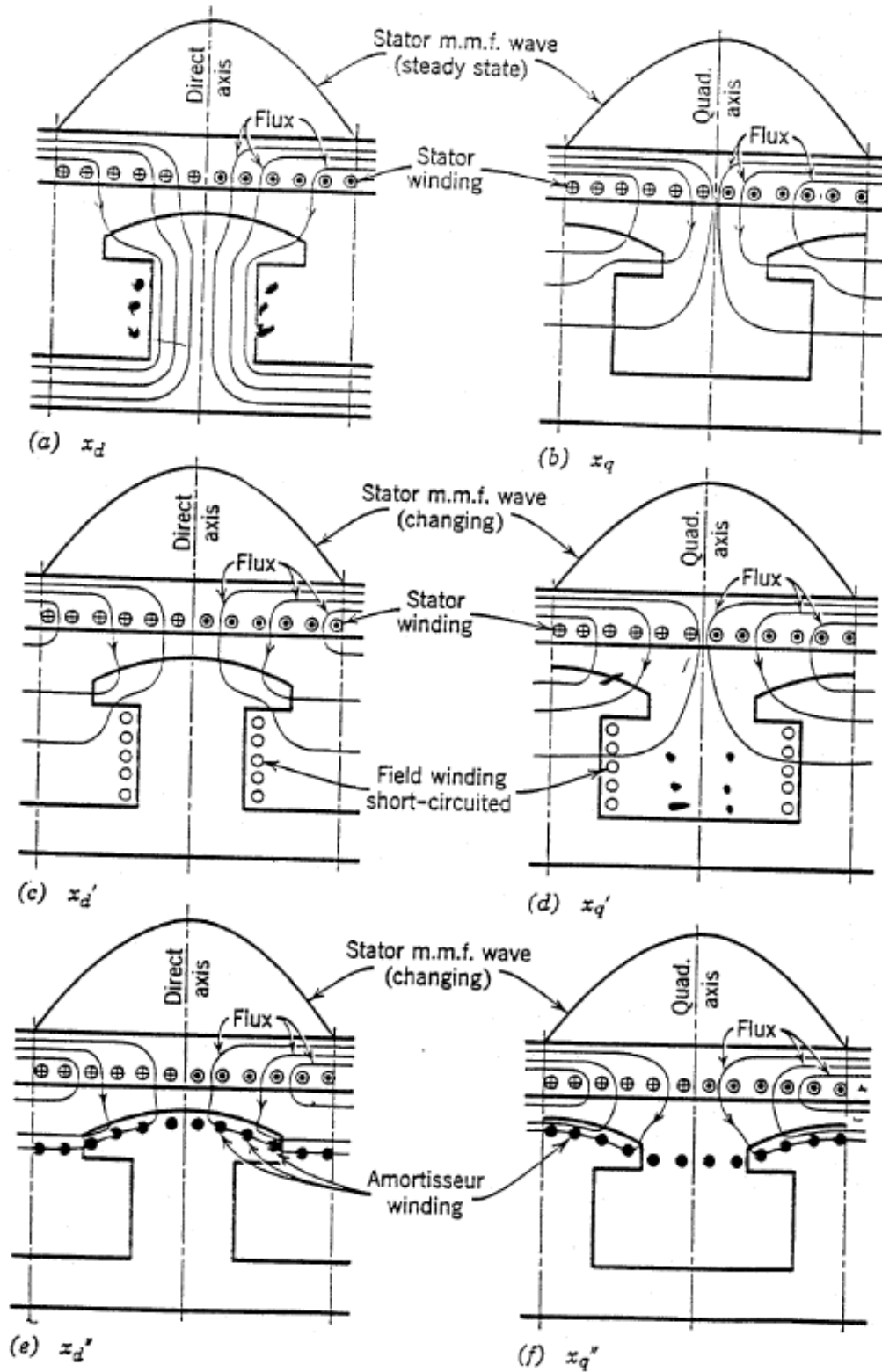


Fig. 15. Flux paths for various reactances of a salient-pole synchronous machine. (a) Direct-axis synchronous reactance. (b) Quadrature-axis synchronous reactance. (c) Direct-axis transient reactance. (d) Quadrature-axis transient reactance. (e) Direct-axis subtransient reactance. (f) Quadrature-axis subtransient reactance. (From Ref. 34 by permission.)

circuits are energized at $t=0$ with a phase that forces the stator MMF wave to be in phase with either the direct-axis or the quadrature axis. Kimbark's picture shows six different figures (illustrating the machine flux paths), one for each of the six reactances that we have identified.

Recall two facts:

1. Inductance is inversely proportional to reluctance: $L=N/R$, where R is reluctance of the flux path.
2. The reluctance of air is much greater than that of a ferromagnetic material.

So let's use the picture to identify the flux path for each of the reactances.

There are five key ideas to be grasped in using these pictures. These ideas help us to understand the flux paths for each different condition. Once we understand the flux paths for each different condition, it will be possible to reason about reluctance, and thus the inductance, of each flux path. Note that the constant flux linkage theorem (CFLT), i.e., no instantaneous change in flux linkage, is central to the thinking of ideas 4 and 5 below.

1. Location of the MMF wave crest relative to the rotor:

In the picture, compare column 1 (Figs. a, c, e) to column 2 (Figs. b, d, f) and note the difference in the location of the MMF wave crest.

- For the purpose of understanding the direct axis inductances, the direct axis flux paths are best visualized when the MMF wave crest is in phase with the direct axis.
- For the purpose of understanding the quadrature axis inductances, the quadrature axis flux paths are best visualized when the MMF wave crest is in phase with the quadrature axis.

The conditions for which the MMF wave crest is in phase with either the direct or quadrature axes are obtained by applying the appropriate a-b-c voltages, as we saw in our "thought experiment" used to derive these various inductances, according to:

- D-axis quantities are obtained from letting $v_a \sim \cos\theta$
- Q-axis quantities are obtained from letting $v_a \sim \sin\theta$

2. Whether flux *can* link with field winding or not:

- Any flux in the D-axis *CAN* link with the field winding: see fig. (a)
- Any flux in the Q-axis *CANNOT* link with the field winding: see fig. (b), (d) and how flux lines are orthogonal to D-axis winding.

3. Whether we analyze with or without damper windings:

This is equivalent to whether we are analyzing after damper winding dynamics have died or before.

- L_d , L'_d , L_q , and L'_q assume no damper windings (after damper winding transients have decayed): see figs (a-d).
- L''_d and L''_q assume damper windings (before damper winding transients have decayed): see figs (e-f).

4. Whether d-axis flux in **F or G field windings** **MUST** be zero (CFLT):

- L_d and L_q characterize the steady-state conditions; here the flux linkage has had time to build up and therefore it links with the F and G windings, respectively – see Figs. (a) and (b). The flux path for assessment of these inductances is “deep” into the rotor circuit.
- L'_d and L''_d are both computed at $t=0+$. Recall that at $t=0$, the flux linkages in the F-winding are zero (no circuit is energized) and because the flux linkages cannot change instantaneously (due to CFLT), these lines of flux *CANNOT* link with the F winding – see Figs. (c) and (e). The flux path for assessment of these inductances is not as “deep” into the rotor circuit as in Fig. (a).
- L'_q and L''_q are both computed at $t=0+$, and because the flux linkages cannot change instantaneously (due to CFLT), these lines of flux *CANNOT* link with the G winding. The flux path for these is not as “deep” into the rotor circuit as in Fig. (b). Special note: The figures were drawn assuming no G-winding (since it is a salient pole machine). Therefore the lines of flux for Fig. (d) (almost like those of Fig. (b)) do appear to exist in the interpolar region where the G-winding would be located. If we did include the effects of the G-winding representation, then Fig. (d) would appear a little more like Fig. (f).

5. Whether d-axis flux in damper windings MUST be zero (CFLT):

- For L_d and L'_d , the d-axis flux has had time to link with the D-winding. see figs. (a) and (c).
For L_q and L'_q , the q-axis flux has had time to link with the Q-winding. See figs (b) and (d)
For both d and q synchronous and transient reactances, the flux paths go relatively “deep” into the rotor.
- For L''_d , which is computed at $t=0+$, the d-axis flux has not had time to link with D-winding. See fig (e).
For L''_q , which is computed at $t=0+$, the q-axis flux has not had time to link with Q-winding. See fig (f).
For both d and q subtransient reactances, the flux paths into the rotor are quite shallow.

The above 5 points should allow us to understand the flux paths for the different conditions illustrated in the different pictures.

From the pictures, we can visually observe whether each flux path appears to be more in the iron (giving low reluctance and high inductance) or air (giving high reluctance and low inductance) and develop “rules” for comparing different data.

Let’s just consider the salient-pole (hydro) machine first.

1. Comparison of d-axis inductances: Observing figs. (a, c, and e), we conclude that the percentage of the path in air (and thus the reluctance) gets increasingly greater with each figure (effects of CFLT), and so the inductance gets smaller with each figure, implying $L_d > L'_d > L''_d \rightarrow X_d > X'_d > X''_d$.
2. Comparison of the q-axis inductances: Observing figs. (b, d, and f), we conclude that the percentage of the path in air (and thus the reluctance) is the same for the steady state and transient periods (because no G-winding), but increases for the steady-state period (because of CFLT),

implying that $L_q=L'_q>L''_q \rightarrow X_q=X'_q>X''_q$. Thus, a useful way to recognize hydro data is that $X_q=X'_q$.

3. Comparison of synchronous inductances: Observing figs. (a, b), we conclude that the steady-state quadrature flux path occurs largely in the interpolar regions and the steady-state direct axis flux path occurs largely in the polar regions, implying that the quadrature flux has significantly more air in its path than the direct axis flux, and therefore quadrature flux path reluctance (inductance) is higher (lower) than direct axis flux path reluctance, so $L_d>L_q \rightarrow X_d>X_q$.
4. Comparison of transient inductances: Observing figs. (c, d), we see that the d-axis path consists largely of the interpolar region whereas the q-axis path consists largely of the polar region, and we conclude that the transient quadrature flux has significantly less air in its path than the transient direct axis flux, and therefore quadrature flux path reluctance (inductance) is lower (higher) than direct axis flux path reluctance, so $L'_d<L'_q \rightarrow X'_d<X'_q$.
5. Comparison of subtransient inductances: Observing figs. (e, f), we see a situation similar to the transient situation, i.e., the d-axis path consists largely of the interpolar region whereas the q-axis path consists largely of the polar region, and we conclude that the subtransient quadrature flux has significantly less air in its path than the direct axis flux, and therefore quadrature flux path reluctance (inductance) is lower (higher) than direct axis flux path reluctance, so $L''_d<L''_q \rightarrow X''_d<X''_q$.

In the case of the round rotor (steam-turbine) machine, number 1 above is the same. The remaining 4 are slightly different, due to the presence of the G-circuit, as follows:

2. Comparison of the q-axis inductances: Observing figs. (b, a modified d, and f), we conclude that the percentage of the path in air (and thus the reluctance) gets increasingly greater with each figure (effects of CFLT), implying that $L_d > L'_d > L''_d \rightarrow X_d > X'_d > X''_d$. So we see that whereas hydro machines have $X_d = X'_d$, the steam-turbine machines have $X_d > X'_d$.
3. Comparison of synchronous inductances: The difference in synchronous inductances for the salient pole machine occurred because of the differences between the polar region and the interpolar region, resulting in $X_d > X_q$. In the round rotor machine, these two regions appear virtually the same, so $L_d = L_q \rightarrow X_d = X_q$. This is another useful way to distinguish hydro data from steam data.
4. Comparison of transient inductances: The same reasoning as in (3) above (for the round rotor machine) would lead us to conclude that $L'_d = L'_q$. This is not the case. The reason is the CFLT requires that the transient flux in each axis **not** link with the F and G-winding, respectively. This effect is more pronounced for the F-winding since it is a “stronger” (more turns) winding than the G-winding. Therefore, q-axis flux goes “deeper” into the rotor, i.e., more of the d-axis flux is forced into the air gap than the G-axis flux. So $L'_d < L'_q \rightarrow X'_d < X'_q$, which is the same for the salient pole machine.
5. Comparison of subtransient inductances: The reasoning of (4) above (for the round rotor machine) would lead us to conclude that $L''_d < L''_q$. This is not the case. The reason is that the damper winding “strengths” are about the same and their effect on each axis is quite similar. So here, we have that $L''_d = L''_q \rightarrow X''_d = X''_q$, although some variation from this rule may occur.

It is interesting to inspect the Diablo Canyon data to see if it conforms to the above rules (it is a steam-turbine machine so we use the second set of rules).

```

UT
NY O
IP W
I      P      TE N X'D X'Q T'DT'Q
MD < NAME ><KV>D<MVA> <F> <#> <> < > < > < > < >
MD DIABLO CYN 211340. 90 1 N PG+ 0.2810.281 430.124

I      P Q MVA      T'D T'Q      SG10 SG12 D
MF < NAME ><KV>D<MVA> <%><%>< ><RA><X'D><X'Q><XD ><XQ >< >< ><XL >< >< >
MF DIABLO CYN 214650.01.01.0134000210.3460.9911.6931.6366.581.5 2280 769 4100.0

```

$$\begin{array}{lll}
 X_d=1.693 & X'_d=0.346 & X''_d=0.281 \\
 X_q=1.636 & X'_q=0.991 & X''_q=0.281
 \end{array}$$

Rule 1: $X_d > X'_d > X''_d \rightarrow$ Yes.

Rule 2: $X_d > X'_d \rightarrow$ Yes.

Rule 3: $X_d = X_q \rightarrow$ Almost.

Rule 4: $X'_d < X'_q \rightarrow$ Yes.

Rule 5: $X''_d = X''_q \rightarrow$ Yes.

One thing to remember: The inductance (reactance) with the smallest reluctance path will be largest.

$$\begin{array}{l}
 X_d > X'_d > X''_d \\
 X_q = X'_q > X''_q \text{ (Salient pole)} \\
 X_q \geq X'_q > X''_q \text{ (Round rotor)}
 \end{array}$$

This is consistent with the figure given at the beginning of these notes (from Kundur, pg. 109) where one can observe that $I'' > I' > I$ where each current is determined by the ratio of a voltage to the appropriate reactance.

Kundur, page 153, provides some comparative data for both salient pole and round-rotor machines (see below).

Also, you can look over some of the data in appendix C of your text to see if it conforms to the above rules.

Table 4.2

SALIENT Round

Parameter		Hydraulic Units	Thermal Units
Synchronous Reactance	X_d	0.6 - 1.5	1.0 - 2.3
	X_q	0.4 - 1.0	1.0 - 2.3
Transient Reactance	X'_d	0.2 - 0.5	0.15 - 0.4
	X'_q	-	0.3 - 1.0
Subtransient Reactance	X''_d	0.15 - 0.35	0.12 - 0.25
	X''_q	0.2 - 0.45	0.12 - 0.25
Transient OC Time Constant	T'_{d0}	1.5 - 9.0 s	3.0 - 10.0 s
	T'_{q0}	-	0.5 - 2.0 s
Subtransient OC Time Constant	T''_{d0}	0.01 - 0.05 s	0.02 - 0.05 s
	T''_{q0}	0.01 - 0.09 s	0.02 - 0.05 s
Stator Leakage Inductance	X_l	0.1 - 0.2	0.1 - 0.2
Stator Resistance	R_a	0.002 - 0.02	0.0015 - 0.005

- Notes:
1. Reactance values are in per unit with stator base values equal to the corresponding machine rated values.
 2. Time constants are in seconds.